Inorganic Chemistry

ARTICLE

pubs.acs.org/IC

Tetrachlorocarbonyliridates: Water-Soluble Carbon Monoxide Releasing Molecules Rate-Modulated by the Sixth Ligand

Damian E. Bikiel,[†] Estefanía González Solveyra,[†] Florencia Di Salvo,[†] Humberto M. S. Milagre,[‡] Marcos N. Eberlin,[§] Rodrigo S. Corrêa,[∥] Javier Ellena,[∥] Darío A. Estrin,[†] and Fabio Doctorovich*[,†]

[†]Departamento de Química Inorgánica, Analítica y Química Física, Facultad de Ciencias Exactas y Naturales, Universidad de Buenos Aires, INQUIMAE-CONICET, Ciudad Universitaria, Pabellón II, C1428EHA, Buenos Aires, Argentina

[‡]Institute of Biosciences, UNESP-Univ. Estadual Paulista, 13506-900 Rio Claro, SP, Brazil

[§]ThoMSon Mass Spectrometry Laboratory, Institute of Chemistry, University of Campinas, UNICAMP, 13083-970, Campinas SP, Brazil

[∥]Departamento de Física e Informática, Instituto de Fisica de São Carlos, Universidad de São Paulo, Caixa postal 369, São Carlos, SP, CEP 13560-970, Brazil

Supporting Information

ABSTRACT: A new family of compounds is presented as potential carbon monoxide releasing molecules (CORMs). These compounds, based on tetrachlorocarbonyliridate(III) derivatives, were synthesized and fully characterized by X-ray diffraction, electrospray mass spectrometry, IR, NMR, and density functional theory calculations. The rate of CO release was studied via the myoglobin assay. The results showed that the rate depends on the nature of the sixth ligand, *trans* to CO, and that a significant modulation on the release rate can be produced by changing the ligand. The reported compounds are soluble in aqueous media, and the rates of CO release are comparable with those for known CORMs, releasing CO at a rate of 0.03−0.58 μM min^{-1} in a 10 μM solution of myoglobin and 10 μM of the complexes.

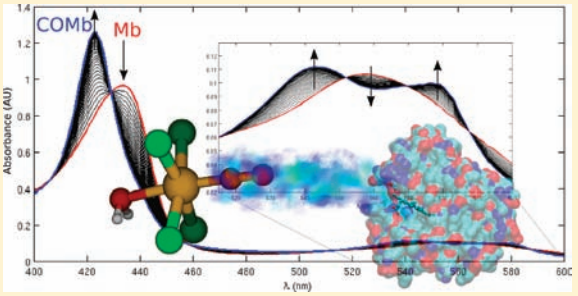

INTRODUCTION

The image of CO as just a noxious gas has been changed to that of an important endogenous biochemical molecule.[1−3] Studies on CO showed vasodilatory, anti-inflammatory, antiapoptotic, antiproliferative, and other pharmacological properties.[4] Human basal production is similar to that of NO, estimated at 20 μmol h^{-1}, which is increased under pathological stages. In recent years, several groups around the world developed different compounds with CO donation capabilities in order to propose new tools for CO physiology experiments. These compounds were named CO releasing molecules (CORMs) by Motterlini et al.[5] The molecules range from boron compounds to transition metal complexes. Regarding the boron compounds, some of them form adducts with CO.[6] For example, $Na[H_3BCO_2H]$ decomposes to CO, H_2, and boric acid under physiological pH and 37 °C with a half-life of 20 min.[7] Several derivatives of this compound were synthesized by esterification and amidation in order to tune the CO releasing rate.[8−10] From an organometallic viewpoint, CO is probably the most important ligand in the chemistry of transition metals. This property was therefore explored by Motterlini et al. in order to develop the first CORMs.[7] The first generation of CORMs involved $[Mn_2(CO)_{10}]$, $Fe(CO)_5$, and $[Ru(CO)_3Cl_2]_2$. Further developments led to $[RuCl(gly)(CO)_3]$, named CORM-3, and related compounds.[7,11] This compound with glycinate (gly) released only one of its CO ligands in water: at 37 °C, the half-life is 98 h; in human plasma, it is reduced to 3.6 min.[2] The use of this compound for biochemical assays is exemplified elsewhere.[7,12−27] Derivatives of the iron compound were also explored: complexes bearing pyrone were recently developed, showing that the releasing rate can be modulated by substitution in the pyrone ring.[28,29] This research was conducted on new compounds involving Fe(II) and Mo(II), which were named CORM-F*: 40 μM CORM-F10 releases (in DMSO), toward a 50 μM myoglobin solution, 3.4 μM min^{-1} of CO in the first 5 min.[30] Other iron compounds were based on cyclopentadienyl and indenyl.[31,32] Releasing experiments involving metallic carbonyls of Cr, Fe, Mn, V, Mo, and W were made in DMSO or ethanol solutions, trying to rationalize the observed releasing rates.[33,34] Cobalt-based compounds have also been explored.[35] Very recently, Zobi et al. reported Re-based CORMs with pH-dependent half-lives ranging 6−43 min.[36] Besides the interest in thermally driven CO release, photoinduced release has also been explored.[37−40] A different approach, using a conjugated hemoglobin-polymer called *Hemospan*, has been shown to have

Received: October 7, 2010
Published: February 15, 2011

potential uses as a CO carrier and delivering agent.[41] Due to the high degree of inertness, some Ir(III) compounds have been studied as therapeuticals.[42,43] In this work, we present a new family of CORMs based on a tetrachlorocarbonyliridate(III) framework. This quite simple moiety has shown to be robust enough to stabilize coordinated S-nitrosothiols, N-nitrosamines, and C-nitroso compounds.[44−48] At the same time, the chloride *trans* to the CO (or N(OR)) moiety is labile enough to be replaced by others ligands.[49] These compounds are soluble in water and release CO under physiological conditions at 37 °C with half-lives on the order of those of known CORMs. The release rate can be tuned by replacing the ligand located *trans* to the CO. Starting with $[IrCl_5CO]^{2-}$, we obtained $[IrCl_4CO(H_2O)]^{-}$ as a product of the hydrolysis in water. We selected pyridine as a prototypical N-based ligand and explored the electronic effects by synthesizing the 4-dimethylaminopyridine derivative. Similarly, we explored another stronger N-based ligand such as 1-methylimidazole. Since each complex holds only one CO ligand, the maximum CO dosage is perfectly known under any experimental condition to be used. Synthesis, structural characterization, and kinetic characterization are described.

METHODOLOGY

All experimental manipulations were performed under anaerobic conditions using standard Schlenk procedures. The $Cs_2[IrCl_5CO]$ complex (**1-Cs**) was synthesized according to the procedure of Cleare and Griffith.[50] K_3IrCl_6, sodium dithionite, and horse heart myoglobin were purchased from Sigma-Aldrich and used without purification. All of the solvents were distilled under N_2 prior to use. In all of the experiments, deionized water was employed.

Instrumental Procedures. Data collection and processing of the X-ray diffraction studies were performed in a Nonius Kappa-CCD diffractometer, with Mo Kα (λ = 0.71073 Å), a graphite monochromator, and T = 298 K. To deal with raw data, the HKL Denzo-Scalepack software package was used.[51,52] All of the reflections were used to obtain the final parameters of the cell. The data were reduced using the DENZO-SMN and SCALEPACK programs. A Gaussian method implemented in WinGX was used for the absorption correction.[53,54] The structures were resolved using SHELXS-97 and were refined with SHELXL-97.[55] All of the non-hydrogen atoms were refined with anisotropic displacement parameters. The hydrogen atoms were located from the difference synthesis of electron density and refined using the riding model on their parent atoms with $U_{iso}(H) = 1.5U_{eq}$ for water and methyl H atoms or $1.2U_{eq}$ for the remaining H atoms.

^1H and ^{13}C NMR spectra were recorded using a Bruker AM500 equipped with a broad-band probe. ^1H and ^{13}C shifts are reported relative to solvent signals with respect to TMS or relative to methanol signals when water was used as a solvent. Correlations were confirmed through HSQC experiments. In the ^{13}C experiments, uncoupling and pulses of 26° were employed.

IR spectra were recorded using a Nicolet Avatar 320 FTIR spectrometer with a Spectra Tech cell for KBr pellets.

Mass spectrometric measurements were performed using a high-resolution hybrid quadrupole (Q) and orthogonal time-of-flight (TOF) mass spectrometer (QTof from Micromass, U.K.) using electrospray ionization in the negative ion mode with potentials from 2100 to 3500 V. Samples dissolved in a methanol/water solution at room temperature (RT) under an inert atmosphere were injected through an uncoated fused-silica capillary, using a syringe pump (Harvard Apparatus, Pump 11, 15 nL min^{-1}). The temperature of the nebulizer and desolvation gas was set at 100 °C, and the cone voltage was set between 25 and 35 V. Tandem mass spectra (ESI-MS/MS) were acquired using the product ion scan mode via selection of the ion of interest, followed by Collision Induced Dissociation (CID) with Ar using energies varying from 15 to 35 eV with high-accuracy orthogonal TOF mass analysis of the CID ionic fragments. For comparison with experimental data, isotopic patterns were calculated using the MassLynx software. Additionally, we performed FT-ICR (Fourier Transform Induced Cyclotron Resonance) measurements. For analysis in both the positive and negative ion modes, pure methanol was used as the spray solvent. Solvents and additives were of HPLC grade, purchased from Sigma-Aldrich, and used as received. Direct infusion automated chip-based nano-ESI-MS was performed on a Triversa NanoMate 100 system (Advion BioSciences, Ithaca, NY) in both the positive and negative ion modes. Samples were loaded into 96-well plates (total volume of 100 μL in each well) and analyzed using a 7.2T LTQ FT Ultra mass spectrometer (ThermoScientific, Bremen, Germany). General ESI conditions were as follows: gas pressure of 0.3 psi and capillary voltage of 1.55 kV and a flow rate of 250 nL min^{-1}. Mass spectra were the result of over 100 microscans processed via the Xcalibur 2.0 software (ThermoScientific, Bremen, Germany).

The elemental CHSN-O microanalysis measurements were obtained using a Carlo Erba EA 1108 system. The analysis was carried out by combustion in a reactor tube and separated by gaseous chromatography in a Paropac column of variable length. The detection was performed via thermal conductivity.

All of the kinetic measurements were carried out on a Hewlett-Packard 8453 diode array spectrometer, equipped with a Lauda RE 207 thermostat. For the hydrolysis experiments, the complexes were dissolved directly in water without pH control (*ca.* 3 mM). The CO releasing experiments were carried out in a phosphate buffer at pH = 7.35 and 0.001 M, with an ionic strength = 0.08 M $KClO_4$. Horse heart myoglobin was used in the experiments. The myoglobin solutions were prepared in a phosphate buffer (*ca.* 10 μM). Sodium dithionite solution was used to reduce the myoglobin prior to each kinetic experiment. For the CO-releasing experiment of **1-Cs**, the initial solution of the complex was added to 9.3× NaCl (for example, 1 mM **1-Cs** + 9.3 mM NaCl) in order to avoid water exchange (*vide infra*). The 4-dimethylaminopyridine (DMApy) derivative was dissolved in DMSO due to its poor solubility in water.

The kinetic data were analyzed by a program written in MATLAB2008a, which allows fitting the experimental data to a particular proposed mechanism. It is composed by a Singular Value Decomposition (SVD) subroutine which extracts the relevant data, diminishing the noise and a minimization subroutine which uses the Simplex algorithm of Nelder−Mean to adjust the proposed kinetic constants.

DFT Calculations. All gas phase DFT calculations performed in this work were carried out using the Gaussian 98 software package. Geometries were fully optimized at the BPW91[56,57] level with a double plus polarization (DZPV) basis set for C, N, O, H, and Cl atoms and the LANL2DZ basis set and effective core potential for the iridium.[58−60] A normal mode analysis was performed in order to obtain vibrational frequencies, force constants, and zero-point energy corrections for the total energy.

Synthesis. The synthesis of the compounds presented in this work has been summarized in a general protocol for clarity. Details regarding each one of the compounds are given in the corresponding paragraph.

General Procedure. A total of 49.5 mg of $Cs_2[IrCl_5CO]$ (**1-Cs**; 663.3 g/mol, 74.6 μmol) was dissolved in 5 mL of distilled and degassed water. The solution was stirred between 1−12 h at room temperature or heated up to 80 °C. Between 1−10 equivalents of the ligand was added, and the solution was stirred for 1−12 h. If the presence of solid was evidenced, the solid was separated by centrifugation and washed with distilled water until reaching a neutral pH. The solid was dried in a vacuum and recrystallized. If no solid was observed, protocol A, B, or C was employed.

Protocol A. The aqueous solution was washed three times with toluene (10 mL) and then one time with dichloromethane. Then,

Table 1. Details of the X-Ray Data Collections and Refinements for 2-As and 4-As

	2-As	4-As
chemical formula	$[Ir\ Cl_4(H_2O)CO]AsC_{24}H_{20}\cdot H_2O$	$[IrCl_4(C_4H_4N_2)CO]AsC_{24}H_{20}$
fw	781.36	827.44
temp (K)	298	298
cryst syst	triclinic	monoclinic
space group	$P\bar{1}$	$P2_1/n$
unit cell dimensions		
a (Å)	11.0493(2)	12.3015(9)
b (Å)	12.0623(2)	18.2647(12)
c (Å)	12.5596(2)	14.5551(7)
α (deg)	111.016(1)	90
β (deg)	95.379(1)	111.975(4)
γ (deg)	111.648(1)	90
vol ($Å^3$)	1402.22(5)	3032.7(3)
Z	2	4
calcd density (Mg/m^3)	1.851	1.812
abs. coeff. (mm^{-1})	6.337	5.863
F(000)	752	1600
cryst size (mm^3)	0.13 × 0.13 × 0.12	0.13 × 0.10 × 0.03
θ range for data collection (deg)	3.01−26.76	2.95−26.39
indices ranges	$-13 \le h \le 13, -15 \le k \le 15, -15 \le l \le 15$	$-15 \le h \le 15, -20 \le k \le 22, -18 \le l \le 18$
reflns collected	10409	30422
independent reflns	5888 [R(int) = 0.0260]	6200 [R(int) = 0.0843]
completeness to θ	98.6	99.8
absorption correction	Gaussian	Gaussian
max. and min. transmission	0.691 and 0.36	0.824 and 0.516
data/restraints/params	5888/0/307	6200/0/344
goodness-of-fit on F^2	1.095	1.036
final R indices [$I > 2\sigma(I)$]	R1 = 0.0348, wR2 = 0.0706	R1 = 0.0398, wR2 = 0.0820
R indices (all data)	R1 = 0.0443, wR2 = 0.0758	R1 = 0.0691, wR2 = 0.0906
largest diff. peak and hole (e/A^3)	0.612 and −1.216	1.012 and −1.528

cosolvent or a saturated solution of tetraphenylarsonium chloride ($AsPh_4Cl$) solution was added. The solution was cooled for 1−6 h, and the solid was centrifuged and dried under vacuum conditions.

Protocol B. A total of 10 mL of dichloromethane was added, and the mixture was stirred for 1 h. A saturated solution of $AsPh_4Cl$ in ethanol was added to the solution and stirred for 1 h. After the separation of the phases, the organic one was washed three times with distilled water and dried with anhydrous sodium sulfate. The filtered solution was concentrated in a rotary evaporator up to 0.5 mL. Cosolvent was added, and the solution was cooled for 1−6 h. The solid was separated by centrifugation and dried in a vacuum.

Protocol C. The solution was concentrated in a rotary evaporator up to 0.5 mL. Cosolvent or a saturated solution of $AsPh_4Cl$ in ethanol was added. The solution was cooled for 1−6 h, and the solid was centrifuged and dried under vacuum conditions.

$(AsPh_4)_2[IrCl_5CO]$ (***1-As***). A total of 60 equivalents of NaCl was added. Once the solids were completely dissolved, $AsPh_4Cl$ (5 equivalents) was added. Then, the solution was evaporated in a rotary evaporator. The orange solid was recrystallized using acetonitrile−toluene. Yield: 60%. υCO FT-IR = 2023 cm^{-1}. Microanalysis: Calcd C = 50.55%; H = 3.46%. Exptl. C = 50.4%; H = 3.8%. ^1H NMR (CD_3CN): 7.91 ppm (tt, 4H), 8.03 ppm (tt, 1H), 7.70−7.80 ppm (m, 16H). ^{13}C NMR (CD_3CN): 151.4 ppm (CO), 135.6 ppm ($AsPh_4^+$), 132.0 ppm ($AsPh_4^+$), 121.0 ppm ($AsPh_4^+$). FT-MS, Calcd: M^-, m/z 441.87; $[M^{2-} + AsPh_4^+]^-$, m/z 776.88. Exptl. m/z 776.88.

$AsPh_4[IrCl_4CO(H_2O)]$ (***2-As***). The solution was heated to 80 °C for 3 h. Then it was cooled to room temperature, and protocol C was followed using 2 equivalents of $AsPh_4Cl$. The orange solid was recrystallized using ethanol−water. Yield: 75%. υCO FT-IR = 2063 cm^{-1}. Microanalysis: Calcd ($+H_2O$) C = 38.4%; H = 3.1%. Exptl. C = 38.2%; H = 3.3%. ^1H NMR ($CDCl_3$): 7.85 ppm (tt, 4H), 7.78 ppm (tt, 8H), 7.63 (dq, 8H), 2.3 ppm (bs, 3H). ^{13}C NMR ($CDCl_3$): 144.6 ppm (CO), 135.3 ppm ($AsPh_4^+$), 133.4 ppm ($AsPh_4^+$), 131.9 ppm ($AsPh_4^+$), 120.7 ppm ($AsPh_4^+$). ESI-MS(−), Calcd: M^-, m/z 376.84. Exptl: M^-, m/z 376.84

$Cs[IrCl_4CO(py)]$ (***3-Cs***). A total of 10 equivalents of pyridine (py) was added. The solution was stirred for 6 h at room temperature. Using protocol A and isopropanol as a cosolvent, a yellow solid was obtained. Yield: 65%. υCO FT-IR = 2085 cm^{-1}. Microanalysis: Calcd C = 12.55%; H = 0.88%; N = 2.44%. Exptl. C = 12.1%; H = 1.2%; N = 2.3%. ^1H NMR (D_2O): 8.95 ppm (dt, 2H), 8.03 ppm (tt, 1H), 7.55 ppm (t, 2H). ^{13}C NMR: 151.2 ppm, 150.5 ppm (CO), 140.5 ppm, 125.5 ppm. FT-MS, Calcd: M^-, m/z 441.87; $[M^- + 2Cs^+]^+$, m/z 707.68. Exptl: m/z 441.87, m/z 707.68.

$AsPh_4[IrCl_4CO(py)]$ (***3-As***). A total of 10 equivalents of py and 10 mL of dichloromethane were added. The solution was stirred for 6 h at room temperature. Protocol B was followed using 5 equivalents of $AsPh_4Cl$ and ethanol as a cosolvent. The solid was recrystallized using dichloromethane−ethanol. Yield: 75%. υCO FT-IR = 2062 cm^{-1}. Microanalysis: Calcd C = 43.70%; H = 3.06%; N = 1.70%. Exptl C = 43.8%; H = 3.1%; N = 1.7%. ^1H NMR ($CDCl_3$): 9.34 ppm (dt, 2H), 7.89 ppm

dx.doi.org/10.1021/ic102038v |*Inorg. Chem.* 2011, 50, 2334–2345

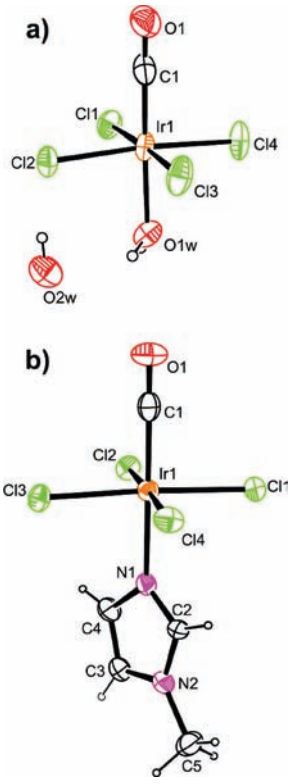

Figure 1. ORTEP diagram at 50% probability ellipsoids for (a) **2-As** and (b) **4-As**. For clarity, only the anion is shown.

(t, 4H), ~7.79 ppm (tt, 1H), 7.78 ppm (t, 8H), 7.63 ppm (d, 8H), 7.37 ppm (t, 2H). ^{13}C NMR ($CDCl_3$): 152.7 ppm (py), 151.9 ppm (CO), 139.0 ppm (py), 135.2 ppm ($AsPh_4^+$), 133.1 ppm ($AsPh_4^+$), 131.2 ppm ($AsPh_4^+$), 124.2 ppm (py), 120.5 ppm ($AsPh_4^+$). ESI-MS(−), Calcd: M^-, *m/z* 441.87. Exptl: M^-, *m/z* 441.87.

Cs[IrCl$_4$CO(1-MeIm)] (***4-Cs***). The solution was stirred for 2 h at 80 °C. A total of 1.2 equivalents of 1-methyl-imidazole (1-MeIm) was added, and the solution was stirred for 30 min. The solution was concentrated in a rotary evaporator. The solids were washed three times with toluene and once with acetone. Yield: 65%. *v*CO FT-IR = 2073 cm^{-1}. Microanalysis: Calcd (+0.33 1-MeIm) C = 12.6%; N = 6.2%; H = 1.30%. Exptl C = 12.3%; N = 6.2%; H = 1.6%. ^{1}H NMR (D_2O): 8.14 ppm (s, 1H), 7.38 ppm (t, J = 1.5 Hz, 1H), 7.11 ppm (t, J = 1.5 Hz, 1H), 3.75 ppm (s, 3H). ^{13}C NMR (D_2O): 152.7 ppm (CO), 139.8 (1-MeIm), 127.2 ppm (1-MeIm), 122.0 ppm (1-MeIm), 34.9 ppm (1-MeIm). FT-MS, Calcd: M^-, *m/z* 444.88; $[M^- + 2Cs^+]^+$, *m/z* 710.69. Exptl: *m/z* 444.88, *m/z* 710.69.

AsPh$_4$[IrCl$_4$CO(1-MeIm)] (***4-As***). The solution was heated for 2 h at 80 °C. After this time, 1.2 equivalents of 1-MeIm was added, and the stirring was continued for another 30 min. Protocol C was followed using 5 equivalents of $AsPh_4Cl$. The solid was recrystallized using dichloromethane−ethanol. Yield: 70%. *v*CO FT-IR = 2052 cm^{-1}. Microanalysis: Calcd C = 42.1%; N = 3.4%; H = 3.2%. Exp. C = 42.4%; N = 3.4%; H = 3.1%. ^{1}H NMR ($CDCl_3$): 8.28 ppm (s, 1H), 7.83 ppm (tt, 4.1H), 7.76 ppm (m, 8.2H), 7.68 ppm (t, J = 1.4 Hz, 1H), 7.59 ppm (m, 8.2H), 6.76 (t, J = 1.6 Hz, 0.9H), 3.64 (s, 2.8H). ^{13}C NMR ($CDCl_3$): 154.4 ppm (CO), 139.1 ppm (Im), 135.0 ppm ($AsPh_4^+$), 132.9 ppm ($AsPh_4^+$), 131.6 ppm ($AsPh_4^+$), 128.5 ppm (Im), 120.3 ppm ($AsPh_4^+$), 119.3 ppm (Im), 34.6 ppm (Im).

DMApyH[IrCl$_4$CO(DMApy)] (***5-DMApy***). Four equivalents of DMApy was added, and the solution was stirred overnight at room temperature. A white-yellowish solid was formed. The solid was recrystallized with dichloromethane−ethanol. Yield: 45%. *v*CO FT-IR = 2054 cm^{-1}. ^{1}H NMR (DMSO-d_6): 8.49 ppm (d, J = 7.5 Hz, 1.7H), 8.10 (m, 1.9H), 6.74 ppm (d, *J* = 7.5 Hz, 2H), 6.60 ppm (m, 2.6H), 3.06 ppm (s, 6H), 2.96 ppm (s, 4H). ^{13}C NMR (DMSO-d_6): 156.4 ppm (CO), 155.1 ppm (DMApy), 150.4 ppm (DMApy), 107.3 ppm (Ir-DMApy), 106.5 ppm (DMApy). FT-MS, Calcd: M^-, *m/z* 484.91; $[DMApyH]^+$, *m/z* 123.08. Exptl: *m/z* 484.91, *m/z* 123.08. Microanalysis: Calcd (+0.5DMApy) C = 33.2%; H = 3.9%; N = 10.5%. Exptl C = 33.0%; H = 3.9%; N = 10.2%.

Table 2. Selected Geometrical Parameters for 2-As and 4-As (Experimental X-Ray Data and DFT Calculations)

	2-As		4-As	
	exp.	calc.	exp.	calc.
d Ir1−C1 (Å)	1.832(6)	1.803	1.854(7)	1.835
d C1−O1 (Å)	1.127(6)	1.167	1.139(7)	1.165
d Ir1−N1 (Å)			2.092(5)	2.129
d Ir1−O1w (Å)	2.110(4)	2.266		
d Ir1−Cl1 (Å)	2.3624(11)	2.442	2.3651(15)	2.444
d Ir1−Cl2 (Å)	2.3392(10)	2.442	2.3585(15)	2.436
d Ir1−Cl3 (Å)	2.3444(12)	2.408	2.3543(14)	2.436
d Ir1−Cl4 (Å)	2.3580(11)	2.408	2.3568(15)	2.444
∠Ir1−C1−O1	178.4(5)	179.5	178.7(6)	180.0

Table 3. Experimental and calculated carbonyl stretching frequencies (cm^{-1}) for the chlorocarbonyliridates presented in this work

	*v*CO (cm^{-1}) experimental	*v*CO (cm^{-1}) calculated
1-As	2023	1990
1-Cs	2065	
2-As	2063	2057
3-As	2062	2057
3-Cs	2085	
4-As	2052	2052
4-Cs	2073	
5-DMApy	2054	2051

RESULTS AND DISCUSSION

X-Ray Diffraction. The crystal data and details of data collection and structure solution and refinement for the crystal structures of **2-As** (CCDC 808951) and **4-As** (CCDC 808952) are summarized in Table 1, while Figure 1 presents the ORTEP diagrams. Tables 2 and 3 show the most relevant geometrical parameters and a comparison to the ones obtained by DFT calculations of the anion. The observation of both structures allows assurance that the *trans* position of the complexes is the preferred one for the substitution. The *trans* effect exerted by the CO ligand labilizes the *trans* chloride in aqueous solution, which is replaced by a water molecule. If a ligand such as py or 1-MeIm is present, the water ligand is displaced, and the corresponding derivatives can be isolated. The most relevant parameters are the Ir−C and C−O distances. The DFT predicted C−O distance for free CO by using the present combination of basis sets and functional is 1.160 Å, while the experimental gas phase value is 1.1282 Å.[61] It can be observed that there exists some differences between the values obtained by X-ray diffraction and the DFT

dx.doi.org/10.1021/ic102038v |*Inorg. Chem.* 2011, 50, 2334–2345

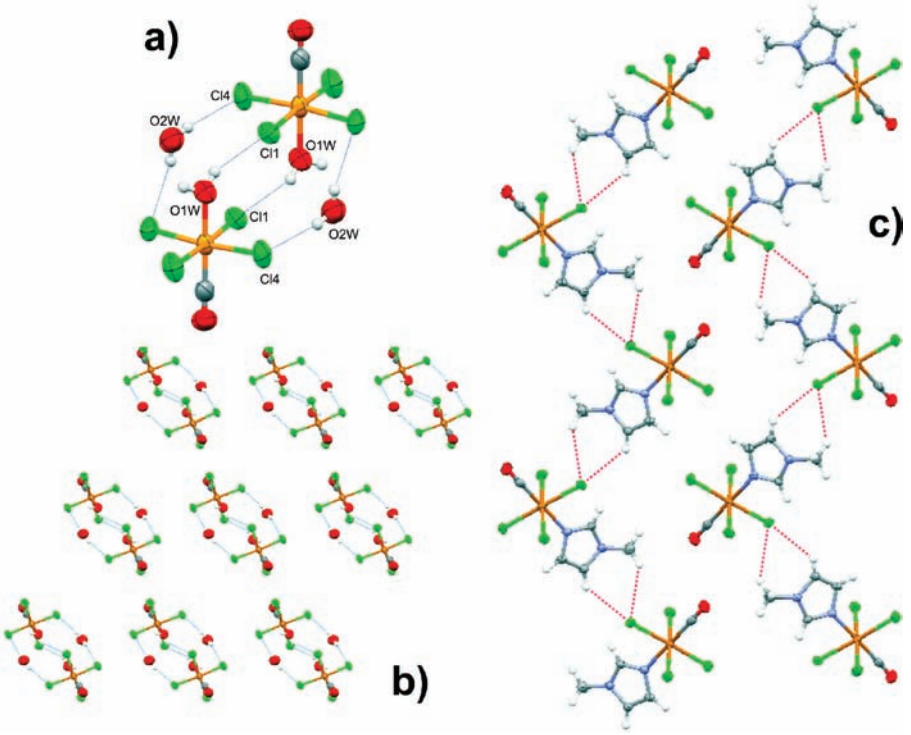

Figure 2. Dimeric supramolecular arrangement observed in **2-As**: (a) O−H···Cl, (b) expanded view, (c) infinite chains are observed for **4-As**.

calculated ones. The X-ray values show a slightly shortened bond for **2-As** and an elongated one for **4-As** (1.127(6) and 1.139(7) Å, respectively, versus 1.1282 Å). Comparison of the calculated C−O bonds of the carbonyls with the one corresponding to free CO shows a slightly elongated C−O distance for **2-As** and for **4-As** (1.167 and 1.165 Å, respectively, versus 1.160 Å for free CO). Analysis of the Ir−C bonds illustrates that DFT predicts correctly the slightly shorter Ir−C bond for **2-As** as compared to **4-As**. Analyzing the experimental X-ray values, it can be observed that, to the contrary of what could be expected, upon elongation of the Ir−C bond (from **2-As** to **4-As**), the C−O bond is also elongated. This fact reflects the poor backdonation from the Ir to the antibonding orbitals of CO. Also, as shown by the DFT calculations, almost no noticeable change in the C−O bond length is observed upon the elongation of the Ir−C bond. Since the effect of the backdonation is to elongate the C−O bond due to the interaction of metal orbitals with antibonding orbitals of the ligand, the behavior is in agreement with a CO ligand interacting mainly as a pure σ donor. Some other Ir(III) carbonyl compounds show similar distances. For example, Ir(COD)-$(CO)_2GePh_3$ presents Ir−C and C−O distances of 1.91 Å and 1.137 Å, respectively.[62] Other Ir(III) complexes such as $[IrCl(CO)_5]^{2+}$ present elongated distances for Ir−C and shortened ones for C−O: 2.02 Å and 1.08 Å, respectively.[63]

Analysis of the supramolecular structure of these compounds shows that while several intermolecular interactions are observed, the CO does not participate directly in any one. In **2-As**, O−H···Cl hydrogen bonds between both water molecules and the Cl ligands give place to the dimeric supramolecular motives shown in Figure 2a and b. On the other hand, an infinite chain as a result of the C−H···Cl intermolecular interactions exhibited in the **4-As** anions is observed (Figure 2c). Finally, some other C−H···Cl interactions, between the phenyl rings from the $AsPh_4^+$ and the Cl, are also present in both structures. Expanded views of both structures as well as complementary crystallographic tables are included in the Supporting Information.

IR. Figure S1 (Supporting Information) shows a typical IR spectrum for the presented family. In particular, the spectrum of **5-DMApy** is shown. The most important features are the signals observed below 1500 cm^{-1}, which correspond to the vibrations of the coordinated DMApy, and the intense band at 2054 cm^{-1}, which corresponds to the CO stretching (υCO). This frequency is in agreement with the values found in terminal carbonyls of transition metal complexes (1820−2150 cm^{-1}).[64−66] As it can be seen in Table 3, the frequency is modified by changing the cation. In all cases, only one frequency compatible with CO stretching was found, confirming that all complexes are monocarbonyl. While for $[IrCl_5CO]^{2-}$ there are no isomeric structures present, for the remaining monocarbonyl complexes, both *cis* and *trans* isomers are possible. Using DFT calculations, we discovered, for all complexes, that the *trans* isomers exhibit υCO 15−30 cm^{-1} higher than the *cis*. In Table 3, we present the calculated *trans* frequencies, which are in good agreement with the experimental ones, **1** being the anion with the larger deviation. Taking into account the X-ray structures for **2-As** and **4-As**, which turned out to be the *trans* isomers, and the experimental and calculated IR frequencies, we propose for the whole family the *trans* configuration. Although the energy differences between both isomers are not very high, this conclusion is reinforced by the fact that the calculated stabilities for the *trans* isomers are higher than for the *cis* ones for all of the complexes in the family (7.3 kcal/mol for **2**, 5.4 kcal/mol for **3**, 4.8 kcal/mol for **4**, and 5.2 kcal/mol for **5**). In the following discussion, we will omit the "*trans*" prefix in the formulas. All compounds have to be thought of as *trans*.

NMR. Probably the most important characteristic of these complexes that can be studied with NMR spectroscopy is the ^{13}C signal due to CO. Using 1D and 2D experiments, we were able

Table 4. Carbonyl ^{13}C NMR Displacements for the Chlorocarbonyliridates Presented in This Work

	δ ^{13}C (ppm) CO	solvent
1-As	151.4	CD_3CN
2-Cs[a]	144.8	D_2O
2-As	144.6	$CDCl_3$
3-Cs	150.5	D_2O
3-As	151.9	$CDCl_3$
4-Cs	152.3	D_2O
4-As	154.4	$CDCl_3$
5-DMApy	156.4	$(CD_3)_2SO$

[a] The spectrum was recorded upon complete hydrolysis of **1-Cs** in D_2O.

to determine the ^{13}C NMR chemical shifts for each carbonyl of the presented complexes. Figure S9 (Supporting Information) shows a 2D experiment performed on **3-Cs**. We employed external 1D experiments in conjunction with HSQC to highlight the quaternary and carbonyl C atoms. In the spectrum, it can be observed that there exists one ^{13}C signal around 150 ppm which does not correlate with any proton signal. Moreover, the remaining ^{13}C signals correlate with H signals. These correlations helped to assign the aromatic hydrogens of the pyridine. Therefore, the noncorrelating signal is assigned to CO. In cases such as the water derivative, the single ^{13}C signal corresponds to CO. The results are summarized in Table 4. The ^{13}C NMR signal for the carbonyl in these compounds was located between 144 and 157 ppm, which resulted in particularly low values: terminal transition metal carbonyls are found in the range 150−220 ppm.[64−66] These rather small differences among the displacements are in agreement with the also small range of observed IR frequencies. The high υCO and the low ^{13}C NMR CO chemical shifts observed are compatible with the poor backdonation present in the compounds.

Electrospray Ionization Mass Spectrometry (ESI-MS). ESI-MS is a powerful technique used to characterize metal transition complexes; consequently, we have used it in previous works to investigate the structures of several classes of such species.[66−71] Being a soft ionization technique, it allows the determination of molecular masses of complex ions and the detection some of the fragments due to the release of ligands. For the studied carbonyl complexes, the presence of the moieties $IrCl_5$, $IrCl_4$, and $IrCl_3$ in the detected signals allows an accurate identification of the corresponding fragments due to their specific isotopologue patterns. The use of high resolution ESI-MS, however, allows unequivocal identification of a fragment formula from its accurate m/z value. Figure S10 (Supporting Information) shows a typical ESI-MS spectrum, in this case for **1**. Note the peculiarity of such MS/MS data where, because of the double charge of the intact parent anion, its signal appears to the left of the spectrum at a low m/z values (m/z 198.89 for the main ion) with the characteristic 0.5 m/z separation for the cluster of isotopologue ions. Upon fragmentation via the loss of a chloride ligand, the $[IrCl_4CO]^-$ ion of m/z 360.82 is obtained, which fragments further by CO loss to form $[IrCl_4]^-$, of m/z 332.82 (and respective isotopologue ions). Note that a further loss of Cl^- would produce the uncharged fragment $IrCl_3$, which is not possible to observe by MS. For all complexes, a similar fragmentation behavior that is fully consistent with the proposed structures as well as their ability to liberate CO was observed, and in addition, the identity of all of the complexes was confirmed by ESI-MS and ESI-MSMS and/or by high resolution FT-MS (Table S12, Supporting Information).

Hydrolysis of 1-Cs. To study the potential capacity of the compounds as CORMs, we checked the stability of **1-Cs** in aqueous solutions. Preliminary experiments suggested that **1-Cs** slowly exchanged ligands in aqueous solutions. In particular, the IR spectra of aqueous solutions showed a υCO shift of ~10 cm^{-1} (see Figure S12, Supporting Information). This result showed that a chloride ligand was replaced by another ligand, probably H_2O. This hypothesis was confirmed by ESI-MS experiments (data not shown) and, furthermore, by the isolation and characterization of **2** using X-ray diffraction and other techniques. Regarding these results, similar behavior was previously observed for $[IrCl_6]^{3-}$, yielding $[IrCl_5H_2O]^{2-}$ and $[IrCl_4(H_2O)_2]^-$ subsequently.[72−74]

The proposed reaction can be described as an associative mechanism:

$$[IrCl_5CO]^{2-} + H_2O \rightarrow [IrCl_5(CO)H_2O]^{2-} \quad (1)$$

$$[IrCl_5(CO)H_2O]^{2-} \rightarrow [IrCl_4(CO)H_2O]^- + Cl^- \quad (2)$$

Assuming that eq 1 is the rate determining step, the rate of the reaction can be written as

$$v = -k[IrCl_5CO^{2-}][H_2O] = -k'[IrCl_5CO^{2-}] \quad (3)$$

where $k' = k[H_2O]$ due to the fact that the reaction is carried out in water. Figure 3 shows a typical kinetic experiment. The changes can be seen in the spectrum due to the modification of the coordination sphere. By using factorial analysis techniques, we obtained from the kinetic experiments the spectra from both species and the concentration profiles (Figure S13, Supporting Information), which allowed us to calculate the kinetic constant at different temperatures. At 298 K, the first order kinetic constant was $(4.28 \pm 0.05) \times 10^{-5}$ s^{-1}, which is comparable but higher than for $[IrCl_6]^{3-}$ (9.4×10^{-6} s^{-1}). The effect of the temperature was analyzed using an Eyring approach. The results can be observed in Figure S14 (Supporting Information). The value for the activation energy (17.5 kcal/mol) is smaller than the one reported for the successive hydrolysis of $[IrCl_6]^{3-}$ (30.4, 29.5, and 30.5 kcal/mol, for the first, second, and third chloride hydrolysis, respectively). The negative value for the activation entropy (−22 cal k^{-1} mol^{-1}) is compatible with an associative process as proposed in eq 1. This result is in agreement with the fact that Ir(III) compounds exchange solvent by associative processes.[75]

Myoglobin Carbonylation Assays. The most popular technique used to evaluate the potential donation of CO from complexes employs myoglobin as the CO trapping agent.[2] In the presence of CO, deoxymyoglobin reacts according to

$$Mb(II) + CO \rightarrow MbCO \quad (4)$$

Deoxymyoglobin yields carboxymyoglobin, which is stable on the time scale of the experiments. In such experiments, changes in the Soret and Q bands are observed. Figure 4 shows the typical plots of CO being released from **2-Cs**.

For each compound, several kinetic runs were recorded, varying the ratio between the complex and the myoglobin. The formation of MbCO was followed at 423 nm, but in each case, the whole spectra were also recorded. The initial rates were obtained by fitting a polynomial function to the first 5% of the trace. For each experiment, the solutions of Mb were thermostatted to 37 °C. Sodium dithionite was then added to reduce the Mb to deoxymyoglobin; the complete transformation was evidenced by the change in the spectrum. Finally, the addition of the carbonyl

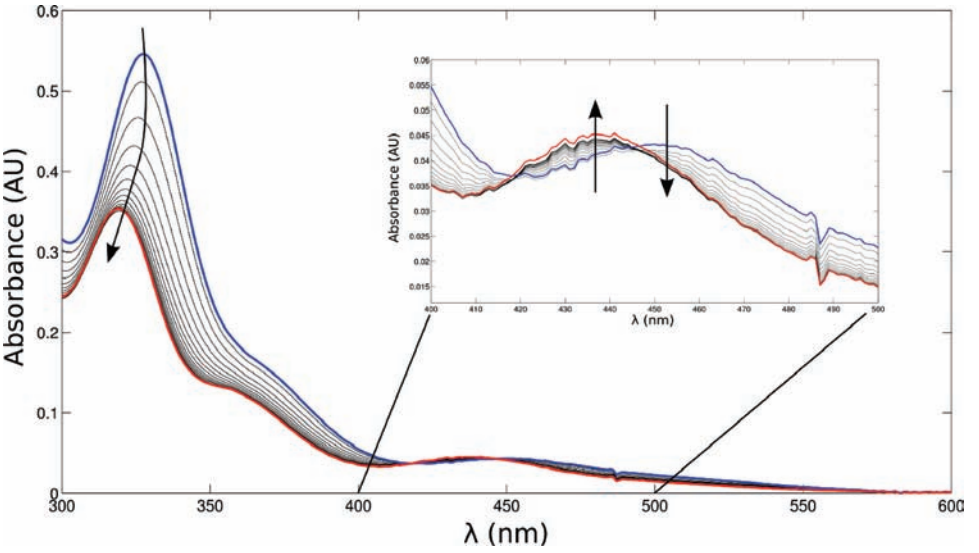

Figure 3. Hydrolysis of **1-Cs** at 333 K. The inset presents a detailed 400−500 nm region.

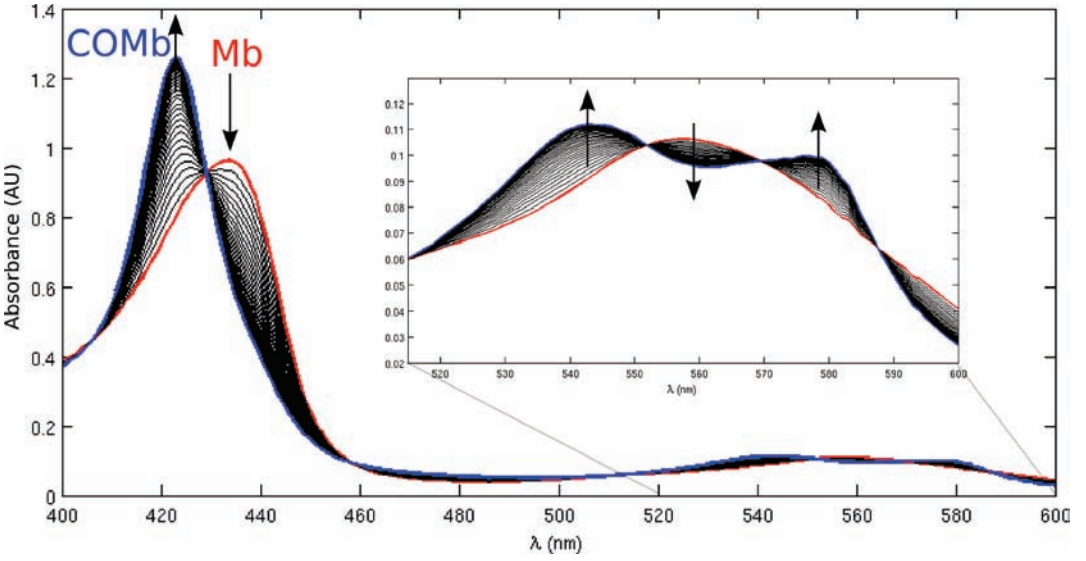

Figure 4. Typical kinetic experiment of CO release (phosphate buffer 0.01 M, pH 7.4, 37 °C) .

complex triggered the reaction. By using the initial rates and plotting against the concentration of the complex, a first order kinetic constant for the observed reaction at initial times can be obtained using linear regression techniques. The same was repeated for the whole family of compounds. By means of initial rate experiments, we were able to show that the rate of carbonylation depends on the CORM concentration (first order), but it is independent of the Mb concentration (Figures S2, S3, and S15, Supporting Information). In Figure S2, the effect on the concentration of the complex is observed. Consequently, upon increasing the concentration, the rate increases. In the same way, the modification of the myoglobin concentration does not affect the initial rate. Besides the completion of the reaction, it can be observed that the three curves presented in Figure S3 are almost similar: the initial slopes are identical.

The initial rate effect upon the change in the concentration of the CORM can be analyzed in Figure S15 (Supporting Information), where a log plot of rate versus concentration is shown. The modification of the rate due to variation of the complex concentration is linear, suggesting that the reaction is first order in the complex, at least at initial times. The compared rates of the complexes can be observed in Figure 5 and Table 5. By using the initial rate release as being indicative of the overall capacity to release CO, the fastest release is observed for **5-DMApy**, while the slowest is for **1-Cs**. However, if the shapes of the releasing curves are analyzed in detail, **4-Cs** shows a particular behavior: after a small initial period, the curve flattens, and eventually, the releasing rate becomes slower than for the chloride derivative. This regime change could be attributed to a competition between the CO and imidazole ligand for the active site of the myoglobin. To test this hypothesis, we repeated these procedures in the presence of imidazole. The experiments were carried out using an excess of complex under the same conditions of pH and temperature of the previous ones. The addition of imidazole gave place to the disappearance of the initial fast regime and a diminution of the slope for the slow

dx.doi.org/10.1021/ic102038v |*Inorg. Chem.* 2011, 50, 2334–2345

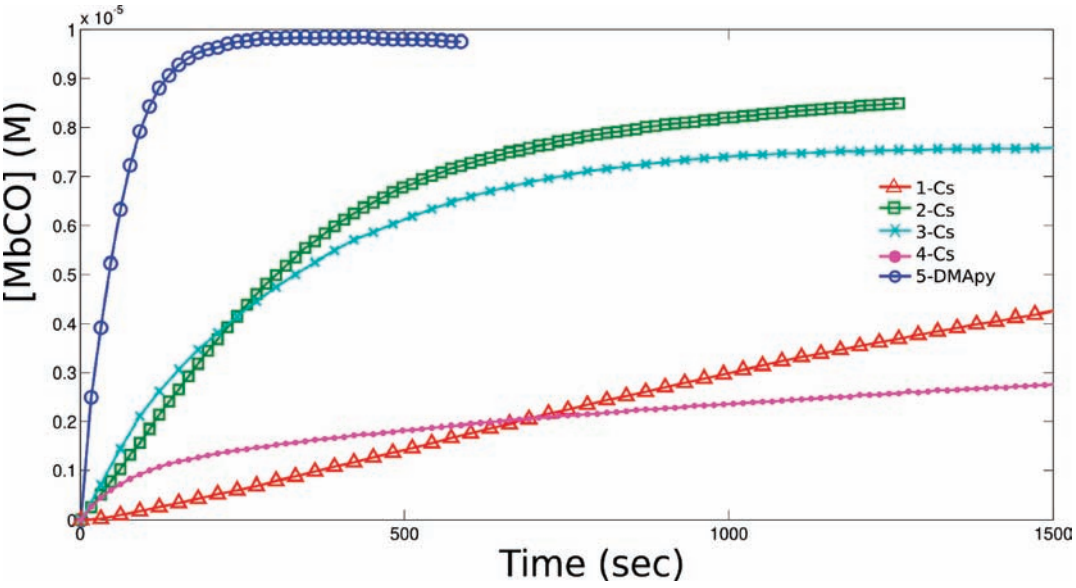

Figure 5. Comparison of the CO-releasing experiments with initial [complex]/[Mb] = 10 for the five anions investigated in this work. The experimental conditions are 0.001 M phosphate buffer, ionic strength of $KClO_4$ = 0.08 M, pH 7.35, 36.5 °C, [Mb] approximately 10 μM.

Table 5. Observed kinetic constants (k_{obs} in s^{-1}) for CO-releasing and initial CO-releasing rates (v_0) for [complex]:[Mb] = 1:1 and [Mb] approx. 10 μM

complex	k_{obs} (s^{-1})	v_0 (μM min−1) complex/Mb ~ 1:1
1-Cs	$(7.5 \pm 0.6) \times 10^{-5}$	0.03
4-Cs	$(11.7 \pm 0.6) \times 10^{-5}$	0.07
2-Cs	$(19 \pm 3) \times 10^{-5}$	0.10
3-Cs	$(26 \pm 1) \times 10^{-5}$	0.09
5-DMApy	$(110 \pm 4) \times 10^{-5}$	0.58

regime (See Figure S16, Supporting Information). Table 5 presents the initial rates of release for all of the compounds, calculated as the amount of CO released during the first minute in a solution containing 10 μM of complex and 10 μM of myoglobin.

It has to be pointed out that the exchange of the *trans* chloride by any of the other ligands produces an increase in the releasing rate of the compound. We can conclude that the decrease in the total charge of the complex facilitates the release of CO, probably due to a decrease in the electronic density available in the metal center to backdonate to the CO. In the same direction, **5-DMApy** is faster than **2-Cs.** The main difference between these two molecules is the potential protonation of the dimethylamino group of the DMApy. At the pH of the experiments and taking into account the fact that upon coordination to a metal center the pK_a of DMApy can be reduced, it is reasonable to suppose that **5-DMApy** is in fact partially or completely protonated. By means of DFT, we calculated the proton affinity for free and coordinated DMApy. We found that ΔG for the deprotonation processes ($DMApyH^+ + H_2O \rightarrow DMApy + H_3O^+$) was equal to 41.2 kcal/mol for free $DMApyH^+$ and 13.8 kcal/mol for the coordinated one. This fact is compatible with the observation of a lower pK_a in case of the coordinated species or, in other words, an easier deprotonation due to coordination. The diminished electronic density of the iridium center in this case can explain the larger releasing rate. If we compare **2-Cs** with **3-Cs**, due to the fact that in these compounds the interaction with the metal is fundamentally σ type (as we discussed in the IR and X-ray sections), there is no fundamental difference between the O or N σ bond, and consequently the rates are almost the same. In Table 6, DFT calculated charges are presented for the metal center and the CO moiety. The effect of the substitution is better observed on the charge developed on the carbonyl. As the Ir−CO bond involves both σ bonding and π backdonation from the metal center to the carbonyl, a net positive charge over the CO represents that σ bonding is more important than the backdonation. While in **1** the net charge is around 0.05*e*, the remaining compounds show a higher positive charge. This is in agreement with the diminished backdonation in the single charged compounds. Using the same analysis, **2** and its deprotonated derivative can be compared. The charge on OH^- is slightly negative, reinforcing the idea of a higher backdonation. When comparing **3** and **5**, both compounds have similar metal and CO charges. However, upon protonation of **5**, the charge on CO increases, confirming that the protonation diminishes the backdonation toward the CO, therefore weakening the Ir−CO bond.

One of the fastest CORMs described in the literature is CORM-F10.[30] The authors report a 3.4 μM min^{-1} releasing rate from a 40 μM solution of the complex in DMSO and 50 μM of myoglobin. This value corresponds to a $t_{1/2}$ of *ca.* 6 min. However, CORM-3 is faster in plasma.[2] Some Mn CORMs with $t_{1/2}$ under 2 min have also been reported.[76] Our fastest complex has a rate that is approximately 70% of CORM-F10 (extrapolating the conditions). The remaining complexes show between 5 and 10% of CORM-F10's releasing rate. Using the kinetic rate constants to compare with the Mn CORMs, our fastest CORM has a $t_{1/2}$ of *ca.* 10 min, and the slowest one is 154 min.

Regarding the mechanism of CO release, the results presented here suggest clearly that the nature of the *trans* ligand affects the rate of donation. The initial rate is independent of the myoglobin concentration and depends linearly on the CORM concentration. These findings are similar to the ones observed in the recently reported Re-based compounds of Zobi et al. Modifications of the *trans* moiety exerted profound changes in the

Table 6. Activation Energies for the Ir−CO and Ir−L Bonds of the Complexes, Calculated at the DFT-BPW91 Level in the Gas Phase and Normal Population Analysis (NPA) Charges for the Ir Atom and CO Moiety[a]

complex	reaction	ΔE (kcal/mol)	NPA qIr (e)	NPA qCO (e)
1	$[IrCl_5CO]^{2-} \rightarrow \{IrCl_4CO\text{----}Cl\}^{\ddagger}$	23.0	0.550	0.045
	$[IrCl_5CO]^{2-} \rightarrow \{IrCl_5\text{----}CO\}^{\ddagger}$	67.8		
2	$[IrCl_4CO(H_2O)]^{-} \rightarrow \{IrCl_4CO\text{----}(H_2O)\}^{\ddagger}$	17.2	0.561 (0.661)*	0.177 (−0.030)*
	$[IrCl_4CO(H_2O)]^{-} \rightarrow \{IrCl_4(H_2O)\text{----}CO\}^{\ddagger}$	75.4		
3	$[IrCl_4CO(py)]^{-} \rightarrow \{IrCl_4CO\text{----}(py)\}^{\ddagger}$	28.1	0.536	0.187
	$[IrCl_4CO(py)]^{-} \rightarrow \{IrCl_4(py)\text{----}CO\}^{\ddagger}$	58.1		
4	$[IrCl_4CO(1\text{-MeIm})]^{-} \rightarrow \{IrCl_4CO\text{----}(1\text{-MeIm})\}^{\ddagger}$	26.8	0.554	0.173
	$[IrCl_4CO(1\text{-MeIm})]^{-} \rightarrow \{IrCl_4(1\text{-MeIm})\text{----}CO\}^{\ddagger}$	61.8		
5	$[IrCl_4CO(DMApy)]^{-} \rightarrow \{IrCl_4CO\text{----}(DMApy)\}^{\ddagger}$	29.1	0.544 (0.530)#	0.176 (0.231)#
	$[IrCl_4CO(DMApy)]^{-} \rightarrow \{IrCl_4(DMApy)\text{----}CO\}^{\ddagger}$	59.5		

[a] A ∗ corresponds to the deprotonated species (OH), and # corresponds to the protonated species ($DMApyH^{+}$).

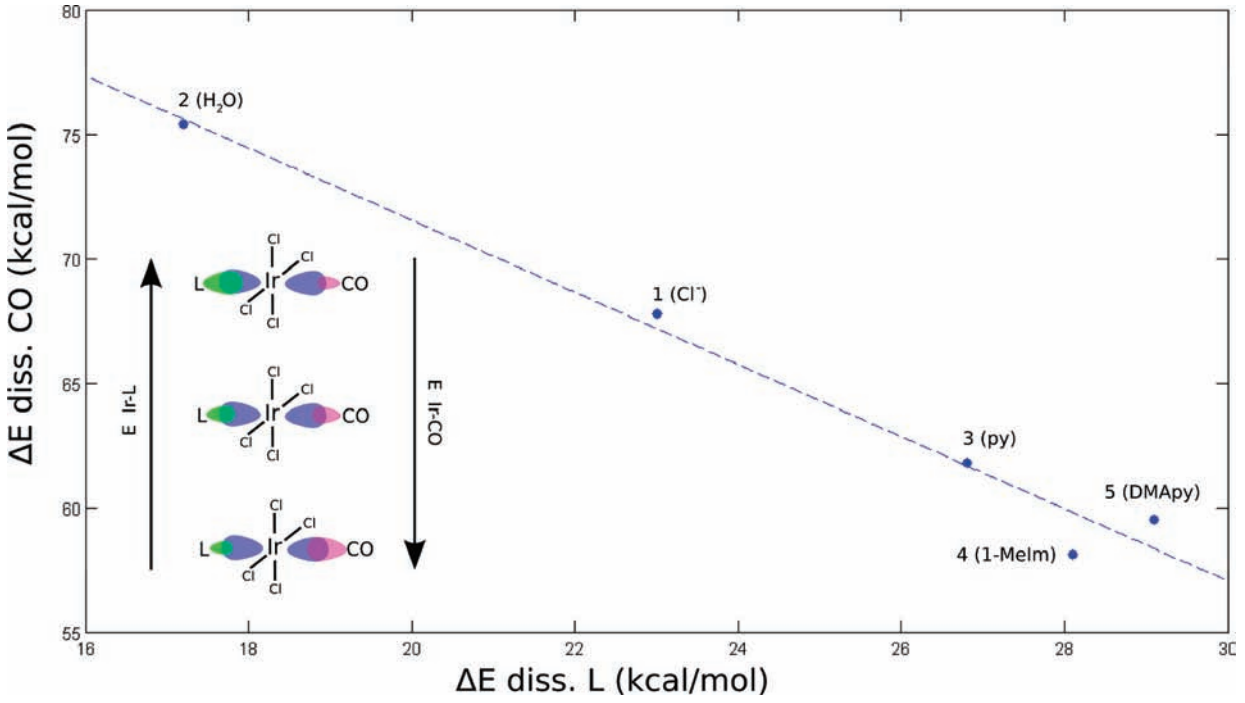

Figure 6. Correlation between the activation energy for dissociation (kcal/mol) of the Ir−CO bond versus the Ir−L bond, calculated at the DFT BPW91 level. The blue line shows the trend.

releasing properties.[36] In summary, the Ir−CO cleavage appears to be the determining step in this type of reaction, at least at initial times. More complex behaviors are observed as long as the reaction continues forward, probably due to competition processes or saturation.

Dissociation Energies Calculated by DFT. Each one of the compounds presented above can exchange both the CO and the *trans* ligand, a fact exemplified by the hydrolysis and the CO release of **1**. The rates for these two processes at 37 °C are $1.24 \times 10^{-4}\ s^{-1}$ (*trans*-Cl^{-} exchange by water) and $7.5 \times 10^{-5}\ s^{-1}$ (CO release in the presence of Mb and Cl^{-}). In order to further explore the influence of the *trans* ligand, we calculated the energy required for the dissociation in the gas phase for both ligands:

$$[IrCl_4CO(L)]^{n-} \rightarrow [IrCl_4(L)]^{n-} + CO \quad (5)$$

$$[IrCl_4CO(L)]^{n-} \rightarrow [IrCl_4CO]^{m-} + L^{p-} \quad (6)$$

For all complexes, we calculated the energy changes associated with reactions 5 and 6. The aim of these calculations is not to describe explicitly the mechanism in solution, but to understand the effect of the *trans* ligand on the CO and vice versa. To estimate this effect, we chose the gas phase activation energy for the ligand dissociation. In order to obtain these magnitudes, we explored the potential energy surface of the dissociation and we performed the explicit search of transition states. In other words, we estimated the activation energy in the gas phase for the cases:

$$[IrCl_4CO(L)]^{n-} \rightarrow \{IrCl_4(L)\text{----}CO\}^{\ddagger} \quad (7)$$

$$[IrCl_4CO(L)]^{n-} \rightarrow \{IrCl_4(CO)\text{----}L\}^{\ddagger} \quad (8)$$

Table 6 presents the calculated energy changes for reactions 7 and 8. It can be observed that, for all anions, the energy required for CO dissociation in the gas phase is higher (58.1 to 75.4 kcal/mol) than for ligand dissociation (17.2 to 29.1 kcal/mol).

dx.doi.org/10.1021/ic102038v |*Inorg. Chem.* 2011, 50, 2334–2345

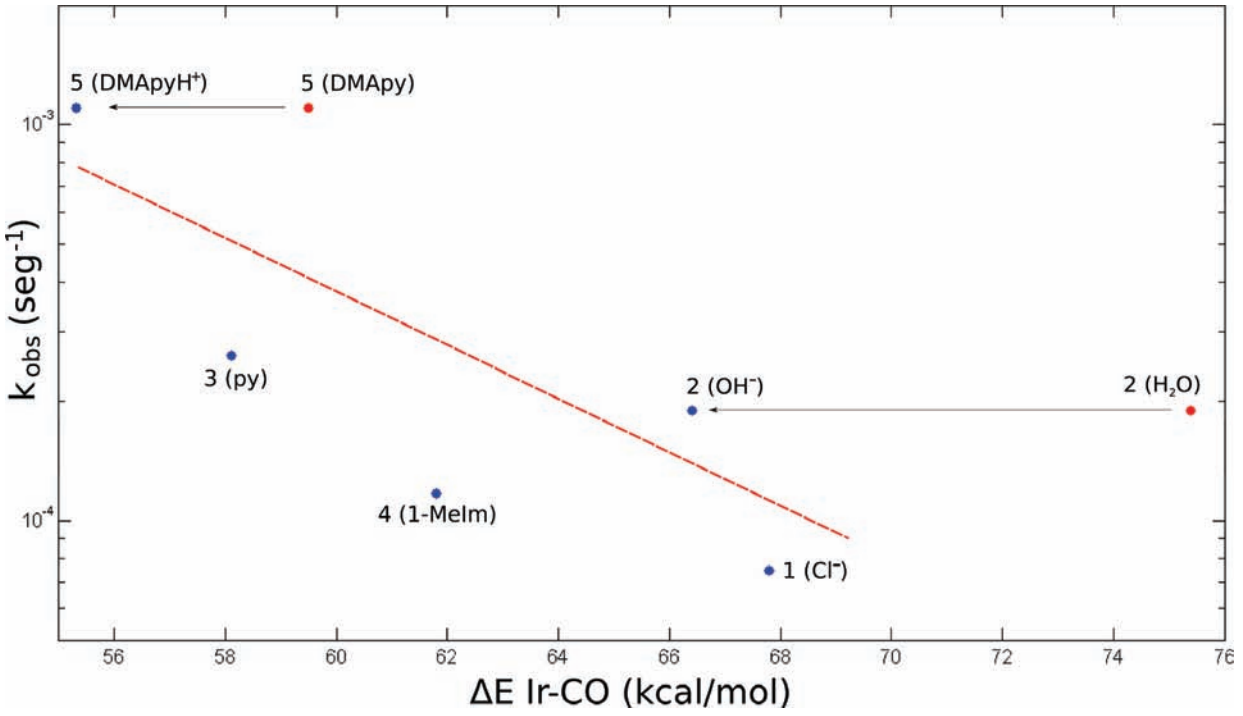

Figure 7. Correlation between the activation (dissociation) energy (kcal/mol) of the Ir−CO bond calculated at the DFT BPW91 level versus the observed kinetic constants for CO release. The red points correspond to H_2O and DMApy complexes (**2** and **5**, respectively). The arrows show the corresponding displacements for the corresponding OH^- and $DMApyH^+$ complexes. The red line shows the qualitative tendency of the points.

Figure 6 presents a correlation between the activation energies of Table 6 for each one of the complexes. It can be observed that the dissociation energies of the Ir−CO and Ir−L bonds are inversely correlated: the complexes with stronger Ir−L bonds present the weaker Ir−CO bonds, and vice versa. These results are in agreement with the almost absent backdonation suggested in these complexes. The particular competition between the *trans* ligands (in this case CO and L) causes the presented trend.

So far, we have presented gas phase calculations while the kinetic measurements were made in aqueous solution. The reactions in solution are complicated due to the interaction of the solvent and pH effects among other variables. Despite the intrinsic nature of the mechanism in solution, we hypothesize that the relative strength of the Ir−CO bond has to contribute, to some extent, to the kinetic behavior of the complexes. Taking into account that the extrapolation from gas phase calculations to the observed kinetic constants in solution should be taken just as a qualitative trend, in Figure 7 we plotted the observed first order rate constants for the releasing compounds (in log scale) versus the corresponding gas phase activation (dissociation) energy. A qualitative trend can be observed: the complexes with the higher dissociation energies are the slower ones. Particularly interesting is the fact that the two points located far from the trend (in red) correspond to the aquo and DMApy derivatives, which probably are the most affected complexes in solution by the acid−base equilibria of the ligands. If we replace the corresponding complexes by the protonated and deprotonated complexes of each one ($DMApyH^+$ for DMApy and OH^- for H_2O), the displacement of their respective points agree with the trend described by the red line (ΔE $DMApyH^+$ = 55.3 kcal/mol and ΔE OH^- = 66.4 kcal/mol; both dissociations coincide with the activations). We can hypothesize that due to the observed kinetic constants, these two complexes are probably in equilibrium between the protonated and deprotonated species, which have different energetics for the CO release. Two important facts can be extracted from these calculations: (1) the strength of the Ir−CO bond can be related to the strength of the *trans* Ir−L bond; (2) a qualitative correlation of the CO releasing rate can be obtained from the Ir−CO dissociation energy.

CONCLUSIONS

A new family of compounds based on $[IrCl_4(CO)L]^{n-}$ was presented. The compounds can donate CO to myoglobin under physiological conditions (aqueous solution, pH 7, 37 °C). The most interesting feature of these species is the poor backdonation from the iridium center to the CO. This effect can be observed in the calculated population (NPA) over the CO moiety in each one of the compounds. The IR and NMR data of the carbonyls spread in a small range, 144−156 ppm for the NMR signals and 2025−2085 cm^{-1} for the IR stretching frequencies. No clear correlations between the stretching frequencies and the NMR signals were found. However, the donation rate is modulated by the identity of the sixth ligand *trans* to CO. The rate is accelerated by almost 20 times when the Cl^- *trans* to the CO is replaced by DMApy. All complexes are soluble in water, and the rates of donation are comparable to other CORMs described in the literature. An inverse correlation between the Ir−L and Ir−CO bonds has been found using DFT calculations, which allows (in principle) one to design *in silico* new potential compounds with higher or lower releasing rates using the qualitative trend observed between the Ir−CO dissociation energy and first order rate constant for CO release. Due to the versatility of the $[IrCl_4(CO)L]^{n-}$ platform, the extension of this family of compounds is easy. Regarding the toxicity of the compounds, while no assays were performed so far, the high degree of inertness of the Ir(III) compounds suggests a low toxicity.

dx.doi.org/10.1021/ic102038v |*Inorg. Chem.* 2011, 50, 2334–2345

■ ASSOCIATED CONTENT

Supporting Information. IR and NMR spectra, kinetic experiments, XRD tables and figures, CIF files. This material is available free of charge via the Internet at http://pubs.acs.org.

■ AUTHOR INFORMATION

Corresponding Author
*E-mail: doctorovich@qi.fcen.uba.ar.

■ ACKNOWLEDGMENT

We greatly acknowledge financial support from Universidad de Buenos Aires (UBACYT X065 and X074), ANPCyT (PICT 2006-2396 and PICT25667), and CONICET (PIP 1207).

■ REFERENCES

(1) Johnson, T. R.; Mann, B. E.; Clark, J. E.; Foresti, R.; Green, C. J.; Motterlini, R. *Angew. Chem., Int. Ed. Engl.* 2003, *42*, 3722–3729.
(2) Motterlini, R.; Mann, B. E.; Johnson, T. R.; Clark, J. E.; Foresti, R.; Green, C. J. *Curr. Pharm. Des.* 2003, *9*, 2525–2539.
(3) Motterlini, R; Otterbein, L. E. *Nat. Rev. Drug Discovery* 2010, *9*, 728–743.
(4) Morita, T.; Perrella, M. A.; Lee, M. E.; Kourembanas, S. *Proc. Natl. Acad. Sci. U.S.A.* 1995, *92*, 1475–1479.
(5) Motterlini, R.; Clark, J. E.; Foresti, R.; Sarathchandra, P.; Mann, B. E.; Green, C. J. *Circ. Res.* 2002, *90*, E17–E24.
(6) Burg, A. B.; Schlesinger, H. I. *J. Am. Chem. Soc.* 1937, *59*, 780–787.
(7) Motterlini, R.; Sawle, P.; Hammad, J.; Bains, S.; Alberto, R.; Foresti, R.; Green, C. J. *FASEB J.* 2005, *19*, 284–286.
(8) Malone, L. J.; Manley, M. R. *Inorg. Chem.* 1967, *6*, 2260–2262.
(9) Carter, J. C.; Moye, A. L.; Luther, G. W. *J. Am. Chem. Soc.* 1974, *96*, 3071–3073.
(10) Hall, I. H.; Rajendran, K. G.; Chen, S. Y.; Wong, O. T.; Sood, A.; Spielvogel, B. F. *Arch. Pharm. (Weinheim)* 1995, *328*, 39–44.
(11) Clark, J. E.; Naughton, P.; Shurey, S.; Green, C. J.; Johnson, T. R.; Mann, B. E.; Foresti, R.; Motterlini, R. *Circ. Res.* 2003, *93*, E2–E8.
(12) Foresti, R.; Hammad, J.; Clark, J. E.; Johnson, T. R.; Mann, B. E.; Friebe, A.; Green, C. J.; Motterlini, R. *Br. J. Pharmacol.* 2004, *142*, 453–460.
(13) Guo, Y.; Stein, A. B.; Wu, W.-J.; Tan, W.; Zhu, X.; Li, Q.-H.; Dawn, B.; Motterlini, R.; Bolli, R. *Am. J. Physiol. Heart Circ. Physiol.* 2004, *286*, H1649–H1653.
(14) Foresti, R.; Shurey, C.; Ansari, T.; Sibbons, P.; Mann, B. E.; Johnson, T. R.; Green, C. J.; Motterlini, R. *Cell. Mol. Biol.* 2005, *51*, 409–423.
(15) Sawle, P.; Foresti, R.; Mann, B. E.; Johnson, T. R.; Green, C. J.; Motterlini, R. *Br. J. Pharmacol.* 2005, *145*, 800–810.
(16) Stein, A. B.; Guo, Y.; Tan, W.; Wu, W.-J.; Zhu, X.; Li, Q.; Luo, C.; Dawn, B.; Johnson, T. R.; Motterlini, R.; Bolli, R. *J. Mol. Cell. Cardiol.* 2005, *38*, 127–134.
(17) Bani-Hani, M. G.; Greenstein, D.; Mann, B. E.; Green, C. J.; Motterlini, R. *Pharmacol. Rep.* 2006, *58*, 132–144.
(18) Bani-Hani, M. G.; Greenstein, D.; Mann, B. E.; Green, C. J.; Motterlini, R. *J. Pharmacol. Exp. Ther.* 2006, *318*, 1315–1322.
(19) Chlopicki, S.; Olszanecki, R.; Marcinkiewicz, E.; Lomnicka, M.; Motterlini, R. *Cardiovasc. Res.* 2006, *71*, 393–401.
(20) Musameh, M. D.; Fuller, B. J.; Mann, B. E.; Green, C. J.; Motterlini, R. *Br. J. Pharmacol.* 2006, *149*, 1104–1112.
(21) Sandouka, A.; Fuller, B. J.; Mann, B. E.; Green, C. J.; Foresti, R.; Motterlini, R. *Kidney Int.* 2006, *69*, 239–247.
(22) Tayem, Y.; Johnson, T. R.; Mann, B. E.; Green, C. J.; Motterlini, R. *Am. J. Physiol. Renal Physiol.* 2006, *290*, F789–F794.
(23) Vannacci, A.; Marzocca, C.; Giannini, L.; Mazzetti, L.; Franchi-Micheli, S.; Failli, P.; Masini, E.; Motterlini, R.; Mannaioni, P. F. *Inflamm. Res.* 2006, *55*, S05–S06.
(24) Musameh, M. D.; Green, C. J.; Mann, B. E.; Fuller, B. J.; Motterlini, R. *J. Heart Lung Transplant.* 2007, *26*, 1192–1198.
(25) Urquhart, P.; Rosignoli, G.; Cooper, D.; Motterlini, R.; Perretti, M. *J. Pharmacol. Exp. Ther.* 2007, *321*, 656–662.
(26) Vannacci, A.; Giannini, L.; Fabrizi, F.; Uliva, C.; Mastroianni, R.; Masini, E.; Motterlini, R.; Mannaioni, P. F. *Inflamm. Res.* 2007, *56*, S13–S14.
(27) Varadi, J.; Lekli, I.; Juhasz, B.; Bacskay, I.; Szabo, G.; Gesztelyi, R.; Szendrei, L.; Varga, E.; Bak, I.; Foresti, R.; Motterlini, R.; Tosaki, A. *Life Sci.* 2007, *80*, 1619–1626.
(28) Fairlamb, I. J. S.; Duhme-Klair, A.-K.; Lynam, J. M.; Moulton, B. E.; O'Brien, C. T.; Sawle, P.; Hammad, J.; Motterlini, R. *Bioorg. Med. Chem. Lett.* 2006, *16*, 995–998.
(29) Sawle, P.; Hammad, J.; Fairlamb, I. J. S.; Moulton, B.; O'Brien, C. T.; Lynam, J. M.; Duhme-Klair, A. K.; Foresti, R.; Motterlini, R. *J. Pharmacol. Exp. Ther.* 2006, *318*, 403–410.
(30) Fairlamb, I. J. S.; Lynam, J. M.; Moulton, B. E.; Taylor, I. E.; Duhme-Klair, A. K.; Sawle, P.; Motterlini, R. *Dalton Trans.* 2007, *33*, 3603–3605.
(31) Scapens, D.; Adams, H.; Johnson, T. R.; Mann, B. E.; Sawle, P.; Aqil, R.; Perrior, T.; Motterlini, R. *Dalton Trans.* 2007, *43*, 4962–4973.
(32) Hewison, L.; Crook, S. H.; Johnson, T. R.; Mann, B. E.; Adams, H.; Plant, S. E.; Sawle, P.; Motterlini, R. *Dalton Trans.* 2010, *39*, 8967–8975.
(33) Zhang, W. Q.; Atkin, A. J.; Thatcher, R. J.; Whitwood, A. C.; Fairlamb, I. J. S.; Lynam, J. M. *Dalton Trans.* 2009, *22*, 4351–4358.
(34) Zhang, W. Q.; Whitwood, A. C.; Fairlamb, I. J. S.; Lynam, J. M. *Inorg. Chem.* 2010, *49*, 8941–8952.
(35) Atkin, A. J.; Williams, S.; Sawle, P.; Motterlini, R.; Lynam, J. M.; Fairlamb, I. J. S. *Dalton Trans.* 2009, 3653–3656.
(36) Zobi, F.; Degonda, A.; Schaub, M. C.; Bogdanova, A. Y. *Inorg. Chem.* 2010, *49*, 7313–7322.
(37) Niesel, J.; Pinto, A.; N'Dongo, H. W. P.; Merz, K.; Ott, I.; Gustb, R.; Schatzschneider, U. *Chem. Commun.* 2008, 1798–1800.
(38) Rimmer, R. D.; Richter, H.; Ford, P. C. *Inorg. Chem.* 2010, *49*, 1180–1185.
(39) Pfeiffer, H.; Rojas, A.; Niesel, J.; Schatzschneider, U. *Dalton Trans.* 2009, 4292–4298.
(40) Kunz, P. C.; Huber, W.; Rojas, A.; Schatzschneider, U.; Spingler, B. *Eur. J. Inorg. Chem.* 2009, 5358–5366.
(41) Vandegriff, K. D.; Young, M. A.; Lohman, J.; Bellelli, A.; Samaja, M.; Malavalli, A.; Winslow, R. M. *Br. J. Pharmacol.* 2008, *154*, 1649–1661.
(42) Messori, L.; Marcon, G.; Orioli, P.; Fontani, M.; Zanello, P.; Bergamo, A.; Sava, G.; Mura, P. *J Inorg. Biochem.* 2003, *95*, 37–46.
(43) Albertí, F. M.; Fiol, J. J.; García-Raso, A.; Torres, M.; Terrón, A.; Barceló-Oliver, M.; Prieto, M. J.; Moreno, V.; Molins, E. *Polyhedron* 2010, *29*, 34–41.
(44) Di Salvo, F.; Estrin, D. A.; Leitus, G.; Doctorovich, F. *Organometallics* 2008, *27*, 1985–1995.
(45) Escola, N.; Llebaría, A.; Leitus, G.; Doctorovich, F. *Organometallics* 2006, *25*, 3799–3801.
(46) Doctorovich, F; Di Salvo, F. *Acc. Chem. Res.* 2007, *40*, 985–993.
(47) Escola, N.; Di Salvo, F.; Haddad, R.; Perissinotti, L.; Eberlin, M. N.; Doctorovich, F. *Inorg. Chem.* 2007, *46*, 4827–4834.
(48) Perissinotti, L. L.; Leitus, G.; Shimon, L.; Estrin, D.; Doctorovich, F. *Inorg. Chem.* 2008, *47*, 4723–4733.
(49) Perissinotti, L. L.; Estrin, D. A.; Leitus, G.; Doctorovich, F. *J. Am. Chem. Soc.* 2006, *128*, 2512–2513.
(50) Cleare, M. J.; Griffith, W. P. *J. Chem. Soc. A* 1969, 372–380.
(51) *Enraf-Nonius COLLECT*; Nonius BV: Delft, The Netherlands, 1997.
(52) Otwinowski, Z.; Minor, W. In *Methods Enzymol.* Carter, C. W., Jr., Sweet, R. M., Eds.; Academic Press: New York, 1997; Vol. 276, pp 307−326.
(53) Farrugia, L. J. *J. Appl. Crystallogr.* 1999, *32*, 837–838.
(54) Coppens, P.; Leiserowitz, L.; Rabinovich, D. *Acta Crystallogr.* 1965, *18*, 1035–1038.

(55) Sheldrick, G. M. *Acta Crystallogr.* 2008, *A64*, 112–122.
(56) Becke, A. D. *Phys. Rev. A* 1998, *38*, 3098–3100.
(57) Perdew, J. P.; Wang, Y. *Phys. Rev. B* 1992, *45*, 13244–13249.
(58) Godbout, N.; Salahub, D. R.; Andzelm, J.; Wimmer, E. *Can. J. Chem.* 1992, *70*, 560–571.
(59) Hay, P. J.; Wadt, W. R. *J. Chem. Phys.* 1985, *82*, 270–283.
(60) Wadt, W. R; Hay, P. J. *J. Chem. Phys.* 1985, *82*, 284–298.
(61) LeFloch, A. *Mol. Phys.* 1991, *72*, 133–144.
(62) Adams, R. D.; Trufan, E. *Organometallics* 2010, *29*, 4346–4353.
(63) Bach, C.; Willner, H.; Wang, C.; Rettig, S. J.; Trotter, J.; Aubke, F. *Angew. Chem., Int. Ed. Engl.* 1996, *35*, 1974–1976.
(64) Spessard, G. O.; Miessler, G. L. *Organometallic Chemistry*; Prentice Hall: New York, 1996.
(65) Crabtree, R. H. *The Organometallic Chemistry of the Transition Metals* Wiley-Interscience: New York, 2001.
(66) Elschenbroich, C.; Salzer, A. *Organometallics: A Concise Introduction*; VCH: New York, 1992.
(67) Toma, S. H.; Nikolaou, S.; Tomazela, D. M.; Eberlin, M. N.; Toma, H. E. *Inorg. Chim. Acta* 2004, *357*, 2253–2260.
(68) Pereira, R. M. S.; Paula, V. I.; Buffon, R.; Tomazela, D. M.; Eberlin, M. N. *Inorg. Chim. Acta* 2004, *357*, 2100–2106.
(69) Toma, S. H.; Uemi, M.; Nikolaou, S.; Tomazela, D. M.; Eberlin, M. N.; Toma, H. E. *Inorg. Chem.* 2004, *43*, 3521–3527.
(70) Alborés, P.; Slep, L. D.; Eberlin, L. S.; Corilo, Y. E; Eberlin, M. N.; Benítez, G.; Vela, M. E.; Salvarezza, R. C.; Baraldo, L. M. *Inorg. Chem.* 2009, *41*, 11226–11235.
(71) Raminelli, C.; Prechtl, M. G. H.; Santos, L. S.; Eberlin, M. N.; Comasseto, J. V. *Organometallics* 2004, *23*, 3990–3996.
(72) Chang, J. S.; Garner, C. S. *Inorg. Chem.* 1965, *4*, 209–215.
(73) El-Awady, A. A.; Bounsall, E. J.; Garner, C. S. *Inorg. Chem.* 1967, *6*, 79–86.
(74) Poulsen, I. A.; Garner, C. S. *J. Am. Chem. Soc.* 1962, *84*, 2032–2037.
(75) Helm, L.; Merbach, A. *Coord. Chem. Rev.* 1999, *187*, 151–181.
(76) Motterlini, R. A.; Mann B. E.; Scapens, D. A. Patent WO 2008/003953.